NOVEL ANALYSIS METHODS TO SUPPORT THE HANDLING QUALITIES EVALUATION OF ROTORCRAFT

Dakota Musso
Resident Engineer
Systems Technology, Inc.
Hawthorne, CA, USA

Emily Vo
Staff Engineer, Research
Systems Technology, Inc.
Hawthorne, CA, USA

Michael Jones
Director of Engineering Services
Systems Technology, Inc.
Hawthorne, CA, USA

David H. Klyde
Technical Fellow
Systems Technology, Inc.
Hawthorne, CA, USA

Joseph Horn
Professor
Pennsylvania State University
University Park, PA, USA

ABSTRACT

Handling qualities (HQ) assessments for rotorcraft are a critical part of the aircraft development cycle. These HQs are often assigned through the use of Mission Task Elements (MTEs) and subjective rating scales using the Cooper-Harper scale. While offline computer simulations continue to improve, pilot feedback during live testing is still required for rating assignment. As the level of autonomy continues to increase, the active role the pilot takes is reduced and objective performance assessment is expected to become more important. New and novel metrics and methods of analysis are needed to support this changing paradigm. This paper introduces novel approach that is designed to aid in the HQ evaluations of VTOL aircraft agnostic to the level of automation. The proposed methodology utilize rainflow counting algorithms to assess vehicle performance during MTEs. The primary advantage of the novel techniques is they were found to provide rapid insight into vehicle performance that is neither strictly time- or frequency-domain based, and can be related back to objective task requirements while showing strong agreement with pilot comments and handling qualities ratings.

NOTATION

*

AAM Advanced Air Mobility

AQTE Automation Qualities Task Element

DI Dynamic Inversion

eCDF Empirical Cumulative Distribution Function

FAA Federal Aviation Administration

HOTL Human On-the-Loop

HOVTL Human Over-the-Loop

HQTE Handling Qualities Task Element

HQR Handling Qualities Rating

HWTL Human Within-the-Loop

MTE Mission Task Element

NASA National Aeronautics and Space Administration

RMSE Root-Mean-Square Error

SAFE Simulation-based Automation and Failure Evaluations

SoS Sum-of-Sines

UAM Urban Air Mobility

VFS Vertical Flight Society

VTOL Vertical Take-Off and Landing

Presented at the 50th European Rotorcraft Forum, Marseille, France, Sept. 10-12, 2024.

1. INTRODUCTION

In recent years there has been a proliferation of new vertical takeoff and landing (VTOL) vehicle concepts, many featuring electric propulsion systems and advanced autonomous capabilities, designed for the advanced air mobility (AAM) marketplace as air taxis and personal air vehicles. Many of these vehicles have flown as scaled proof of concepts, while several others are now flying as full-scale prototypes. These vehicles almost exclusively feature fly-by-wire flight control systems including advanced control modes (i.e., response augmentation), increased automation, and autonomous systems of varying levels. Following the Simplified Vehicle Operations (SVO) as defined in (Ref. 1) and progression of the Urban Air Mobility (UAM) Maturity Levels (UML), technological, infrastructure, and certification advancements are required to ultimately lead to fully autonomous operations. Because of the complexities involved in control system design, autonomous systems, and operating environments, new certification means of compliance methods are needed to ensure safe operations within the national airspace, especially dense urban environments.

Traditional methods of handling qualities evaluations such those provide by the Mission Task Element (MTE) approach laid out by ADS-33E-PRF (Ref. 2) (recently superseded by MIL-DTL-32742 (Ref. 3)) have long been used by aircraft designers. These approaches have an excellent track record and provide a proven methodology for systematically comparing and evaluating rotorcraft HQs in a variety of conditions. The Federal Aviation Administration (FAA) has begun adopting MTEs as a possible means for certification in civilian aircraft through the use of so-called Handling Qualities Task Elements (HQTEs) (Ref. 4). As the AAM market matures, there will likely be increasing use of autonomy, where the level of pilot interaction with the system progresses from human-within-the-loop (HWTL) to human-on-the-loop (HOTL) and finally human-over-the-loop (HOVTL). At each level, the human pilot is less responsible for the actual "flying" of the aircraft. As such, pilot feedback during evaluation becomes increasingly challenging to obtain, and with fully autonomous operation it may eventually be impossible to obtain. Figure 1 shows a schematic of the envisaged progression in assessment methodology as certification efforts move from HWTL systems to HOVTL. These are only considered only as broad estimations of how the assessment will change. As automation increases, objective performance assessment is expected to become more important, whereas the pilot feedback plays less of a role. The automation trust starts to become important and the feedback from the operator or occupant. As vehicles become fully autonomous (HOVTL), assessment, ride qualities, trust, and operator feedback are important, and the feedback of the 'pilot' is no longer required.

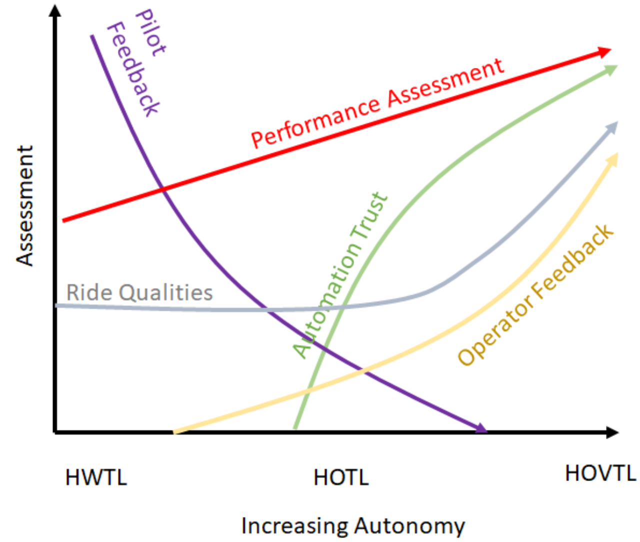

Figure 1. Assessment Methods with Increasing Autonomy

Recent advancements in simulation capabilities and tools have allowed MTE/HQTE evaluation to take place using an analytical model through the use of the Task-Pilot-Vehicle approach (Refs. 5, 6). While these tools and techniques are very promising in their utility to evaluate aircraft HQs in early design stages, they can also suffer from a lack of pilot feedback when an automated "pilot" is used to control the vehicle.

There are many metrics that can go along with the MTE/HQTE approach that have been shown to be effective. Scores computed based on the duration the vehicle spends in the adequate/desired/no-go regions of different portions of the tasks are part the requirements laid out by ADS-33 and MIL-DTL-32742. Time-based metrics such as root-mean-square error (RMSE) have been shown to have a strong correlation between predicted and actual handling qualities and workload ratings (Refs. 7, 8). Frequency domain techniques have been successfully applied to this problem as well. For closed-loop compensatory tracking tasks (such as Sum-of-Sines) pilot-describing functions can provide a wealth of information about the interactions in the pilot-vehicle system (Ref. 9). Finally, hybrid frequency/time domain methods, such as the attack metric (Ref. 10) and scalogram based approaches (Ref. 11) can inform about pilot activity-on-the-stick, and used to identify portions of the task that correspond to increased workload in both piloted (Ref. 12) and automated (Ref. 6) task execution.

While often effective in the process of HQ evaluations, some of these metrics rely heavily on pilot feedback to provide the necessary context, other metrics might only work for specific tasks or can only be interpreted properly when applied to vehicles with specific levels of autonomy. It is therefore important that metrics be developed that are agnostic to not only the level of autonomy, but also the availability of pilot feedback.

In that light, a novel analysis method to support HQ evaluations is proposed based on rainflow counting that can work at any level of vehicle autonomy. Rainflow counting (Ref. 13) (also known as cycle counting) is a common set of algorithms used in the process of fatigue life computations of a component subjected to uni-axial loading sequences and provides the quantification of stress cycles via time history load data (Ref. 14). The method extracts the sub-cycles from a time series of stress data and counts the number of closed loop cycles with a given mean and range (Ref. 15). Although this algorithm is traditionally applied to the field of material science for cyclic fatigue analysis, damage assessment of components based on crack growth (Ref. 16) and as an aid in vibration analysis of materials (Refs. 17,18), applications are also observed in the electrical and biomedical fields. Uses regarding battery and device lifetime estimation (Ref. 19) and analysis on time-varying biological data (Ref. 20) prove the versatility of the algorithm. Of the existing studies, the rainflow counting technique is applied to time-varying properties of a subject to assess the current state or predict the future state. The authors have been unable to find any studies to-date in which rainflow counting algorithms are utilized to assess the behavior and performance of an aircraft system.

The paper proceeds as follows. Section 2 provides an overview of the project that enabled the development of the novel metrics. Section 3 gives a description of the facility, aircraft model, and control system. Section 4 gives details of the development of the novel metrics. Section 5 presents the results of the piloted simulation studies and the analysis using both traditional and the newly proposed methods. Finally, Section 6 offers concluding remarks and implications for future work.

2. S.A.F.E. PROCESS

As the UAM market continues to evolve, a reliable and repeatable process is needed that can help provide a means of compliance certification method for autonomous systems including degraded modes that is safe, repeatable, and discriminating. Systems Technology, Inc. has been working with NASA to develop a Simulation-based Automation and Failure Evaluations (SAFE) process to achieve this end. This work has been funded through a NASA Small Business Innovation Research (SBIR) Phase II research program. The feasibility of the SAFE process has been demonstrated via piloted simulations using an AAM-representative VTOL lift plus cruise vehicle real-time model.

Using the mission task element approach as a certification means of compliance (Ref. 21), the SAFE process is used for the exploration, development, and testing of new handling qualities task elements (HQTEs) and automation qualities task elements (AQTEs) as illustrated in Figure 2.

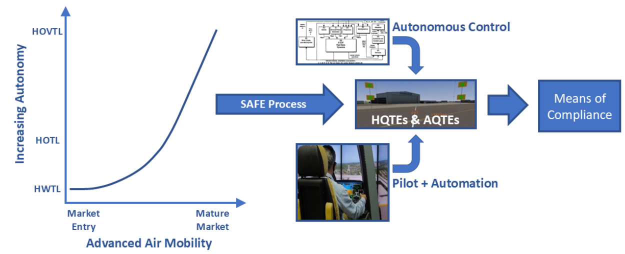

Figure 2. SAFE Process for Advanced Air Mobility Means of Compliance Testing

One of the primary benefits of the SAFE tool is that it provides a structured framework that removes all guesswork during the HQTE evaluation process. This means less time is spent setting up the process, giving more available time to the exploration of novel metrics, improvements to the vehicle, or even improvements to the HQTEs themselves.

2.1. Application Overview

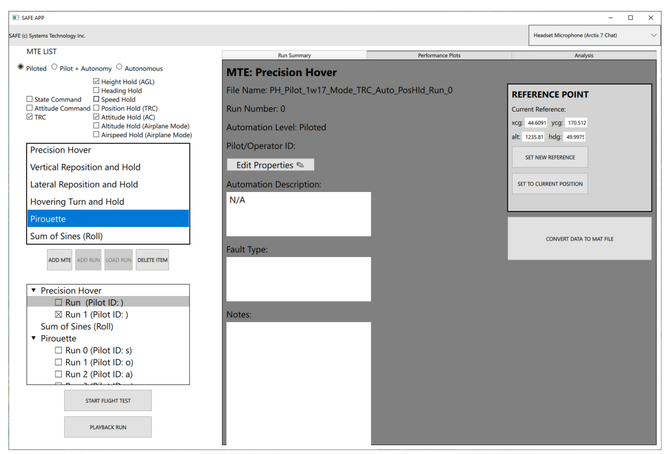

Figure 3. SAFE Application – Task Card View

The SAFE process is intended to guide the user through the HQ evaluation process by constructing and dictating the test plan based on given requirements through a tablet-based application which provides live analysis, data collection, and playback geared toward simulated flight tests. The 'Initial Conditions' set the parameters for the three subsequent stages of the tool. At this point, the level of automation is selected, mission requirements and test rationale. Then relevant test cards, HQTEs, and assessment tools are selected. These are selected

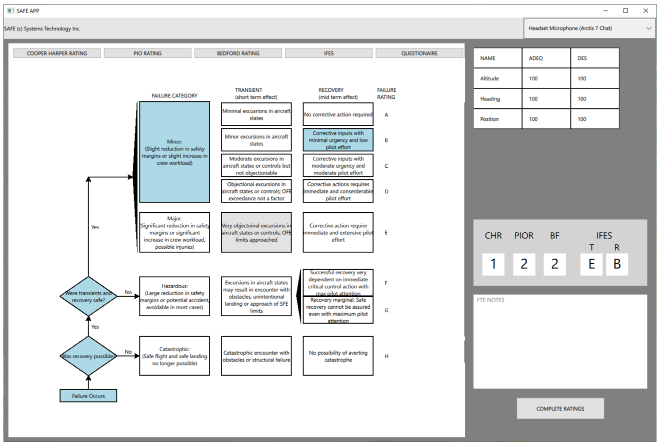

Figure 4. SAFE Application – Rating Scale View

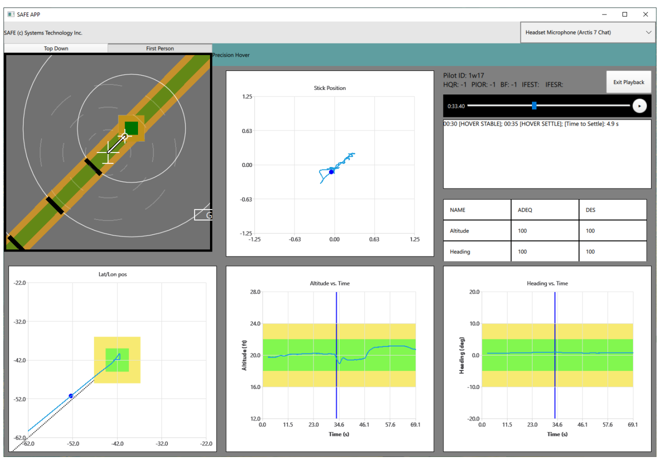

Figure 5. SAFE Application – Playback View

based on the initial conditions, which therefore provides a standardized process for the assessment. This eliminates the need for subjective selection of assessment methodologies. The selected elements are used in the real-time test, which is used to collect and process data during the flight or simulator testing. The real-time test is used to save data, collect pilot comments and to objectively evaluate the task performance. In addition to presentation of after run task performance assessments, the collected material is saved for post-processing.

The application lets users set up a test campaign featuring Mission Task Elements (MTEs) either before or during the simulated flight tests. Each run is logged into the application with corresponding information such as automation level, mode, faults, and other additional notes, essentially creating a digital run log (see Figure 3). During a run, the application provides live time aircraft state views, performance plots, and performance calculations tailored to each MTE. The live plots and performance calculations provides both engineers and the pilot immediate feedback on the task performance. This feature helps pilots better gauge their own performance during practice runs before scoring a run, and helps the engineers adjust the test plan as indicated by the pilot's performance. The SAFE application also provides the ability to visualize and store ratings such as the Cooper Harper Ratings (HQR) (Ref. 22), Bedford Workload Rating scale (Ref. 23), Pilot Induced Oscillations Ratings (PIOR) (Ref. 24), and the Integrated Evaluation Failure Scale (IFES) (Ref. 25) for each run (see Figure 4). A customizable survey is also available for pilots to provide feedback on the runs. While the run takes place, the application records the data being streamed to it. With the recorded data, the SAFE application features a "playback" option as shown in Figure 5, in which runs can be replayed (including available audio data), a feature especially helpful during post-test debriefing and analysis.

Users of the application are also given the ability to immediately run analysis on completed runs using MATLAB functions, providing analysis such as root mean square error values, Rainflow Counting values and plots, and pilot describing functions. The SAFE process provides quick performance calculations, analysis, and detailed run logging. Usage of this process for a simulated test campaign demonstrated that the process is beneficial during and after the trials. The SAFE process can quickly reveals deficiencies in the test plan during tests, and records critical information for post-test analysis.

2.2. Developmental Tools

The SAFE application is developed with Qt (Ref. 26). Qt is a cross-platform development tool used for creating graphical user interfaces (GUI). Qt/QML features portability (ability to be deployed onto platforms of different OS) which suits SAFE's tablet platform. While the visual GUI and event handling is composed through QML, the data management is performed through C++ code. External MATLAB functions accessed via the MATLAB Engine API are employed for additional in-application analysis. The SAFE app can be fully packaged and deployed independent of Qt Creator IDE, and onto other devices.

The SAFE system currently supports 7 different MTEs: Precision Hover, Lateral Reposition, Vertical Reposition, Hover Turn and Hold, Pirouette, Sum of Sines, and Heliport Approach. These courses are built in the application using Qt Quick 3D for visualization purposes during the runs. The benefit of using Qt Quick 3D is its ability to leverage the static component of all the MTE 3D courses. A single 3D course is generated for each MTE course, the camera is then positioned and altered to provide multiple views of the static scene. During runs of flights and in playbacks of the flight, the user is given the option to view the aircraft performing the MTEs either a first person point of view with a primary flight display, or from a top down point of view with an ownship and hover cue. The visualization of the aircraft and courses provides the engineers a clear connection between the data plotted and the aircraft state. These 3D courses are easily manipulated to match the simulation environment; furthermore, giving opportunity to create new or custom tasks.

2.3. Data Connection Setup

SAFE receives data from the flight simulator via User Data Protocol (UDP), a basic communication protocol used to transfer data within an IP network. For the communication setup, the simulation environment and SAFE are required to be on the same network. The required signals from the simulation environment are transferred to the SAFE application via UDP in the form of data packets composed of the simulation's live signals. Since there is no dependency from the simulation environment on the SAFE application, usage of the SAFE application does not affect the simulation. The simplicity of this communication setup allows for the SAFE application to be versatile for usage in various simulation environments.

SAFE also provides consistency between the virtual courses in the simulation environment and the plots/visuals in the application. To link SAFE with the visual courses in the simulation environment, a common positional reference point system is used to ensure that the SAFE course is synced with the simulation environment's course. The process involves flying the simulated aircraft to the final hover point of the HQTE with the SAFE application running. Once at the hover point, the application pulls the current aircraft position, altitude, and heading for the reference. For a single test campaign, the reference positions remains consistent for each HQTE. Since the positional references are already accounted for in the data collected by SAFE, external analysis of the positional data does not require further adjustments for reference position. Setting the reference position does not require a trained pilot, so this process can be performed prior to formal testing.

3. SIMULATION ENVIRONMENT

Piloted simulation was conducted at the Rotorcraft Simulation Facility at Pennsylvania State University (Figure 6). The simulation facility features:

- BA 609 Cab (standard cyclic, collective, pedals with option for side-stick controller).
- 5m diameter spherical screen with 210° HFOV / 70° VFOV.
- Six-channel projection system (seamless blend/warp, auto-calibration using NWarp).
- 23-inch touchscreen displays with programmable instrument displays using VAPS-XT.
- Fully programmable, 4-axis control loading system.
- 6-DOF motion base, ±6 inches of translation, ±25 degrees of angular displacement (motion base was not used for this study).

Figure 6. Penn State Rotorcraft Simulation Facility

The 4-axis control loading system has the capability to provide active force-feel feedback to a conventional center cyclic stick, a collective stick, and pedals. Several buttons and toggle switches are available on the various sticks and can be used for additional control inputs (e.g., pusher propeller control) or additional controller functions (e.g., mode selection). The touchscreen interface can also be used by the pilot for control mode selection.

The Penn State flight simulator uses the X-Plane commercial simulation software for out-the-window displays. X-Plane is used solely as a graphics engine, while external codes are used to drive the flight dynamics. The X-Plane visual database in the Penn State simulator contains virtual HQTE courses to facilitate piloted evaluations. An example virtual courses is shown in Figure 7.

3.1. AAM Vehicle Model

The AAM configuration for the study is an electric Vertical Takeoff and Landing (eVTOL) aircraft with a Lift + Cruise configuration. It is capable of vertical flight and conversion to a fixed-wing configuration in high-speed flight. The specific configuration is a 7,000 lbs aircraft referred to as PSU Reference Aircraft #2, as described in a recent paper (Ref. 27) and shown in Figure 8. The aircraft configuration and sizing are similar to the Beta Technologies ALIA aircraft. However, the aircraft is entirely generic. For example, the detailed aerodynamic properties (e.g., airfoils, blade planform and twist) are

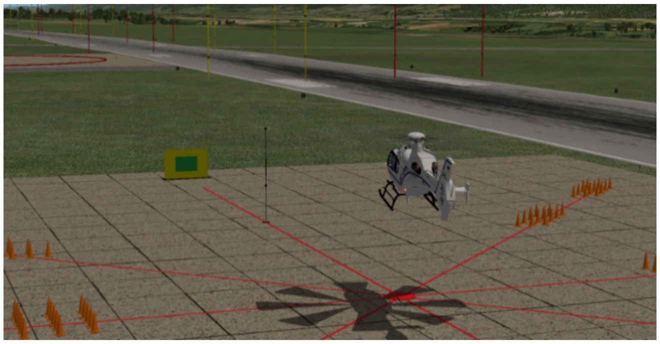

Figure 7. Example Hover Course in PSU Simulator

all notional, and some features, such as the sizing and number of blades on the cruise propeller, differ significantly from published data on the ALIA.

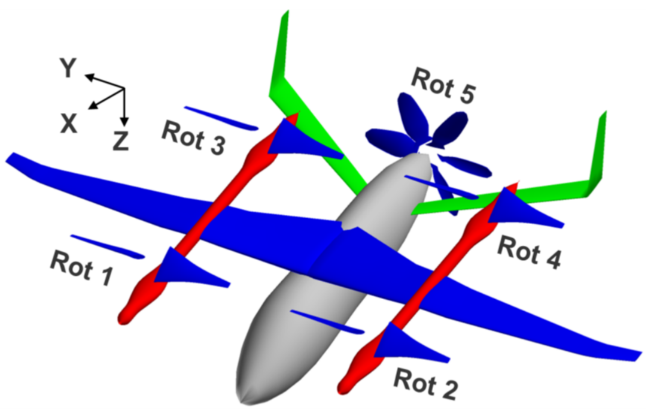

Figure 8. PSU Reference Aircraft #2

The aircraft is modelled using the PSU-DEPSim software, which is described in detail in (Ref. 28). PSU-DEPSim provides a complete state-space representation of the non-linear equations of motion, rotor blade dynamics, finite-state rotor inflow, electric motor dynamics, and actuator dynamics. The simulation is developed in the MATLAB / Simulink environment and is executable in Simulink or auto-coded to C and executed in real-time via a wrapper code. Rotors can be modelled via a complete blade element model with look-up tables for blade aerodynamic coefficients, or via a simplified actuator disk model that assumes linear lift slope and uses an approximate analytic integration of rotor forces over a revolution. Both rotor models have the option of including blade flapping dynamics or they can be assumed rigid. Wings and tail surfaces are modeled using a strip theory with look up tables for aerodynamic coefficients at each segment and finite-wing corrections. PSU-DEPSim has the option to model the motors via an 8-state model of a 3-phase electric motor, or alternatively they can be modeled using a simple 1st order torque model. The motors models include an RPM controller such that rotor speed follows an RPM-command reference model.

The model also includes a real-time capable rotor-to-rotor and rotor-to-lifting surface interference model using the Combined Momentum Theory and Simple Vortex Theory (CMTSVT) model (Ref. 29). The model links the finite-state inflow models between lifting rotors to account for aerodynamic interactions. It can also compute induced velocities on the wing and tail sections.

For the study reported in this paper, the lift rotors are modelled using an actuator disk model of a rigid rotor, while the pusher propeller is represented by a blade element model of a rigid rotor. The 3-phase electric motor model is used for all motors, with prescribed torque limits approximately equal to two times the lift rotor torque required for hover trim. In the simulation, only a single motor is modeled per rotor system. When fault cases are addressed later in the study, motor failures will be modelled by cutting the torque limits by 50%. First order actuator models are used with a bandwidth of 40 rad/sec.

In hover, the aircraft uses variable RPM on the lift rotors for primary control of all axes (i.e. it uses quad-rotor type control mixing). As the aircraft transitions to forward flight airspeed above 70 knots, the lift rotor RPM is steadily reduced until they are shut off completely at 85 knots. Above 85 knots, control is achieved entirely via fixed-wing control surfaces (ailerons, elevator, and rudder) and via the pusher cruise propeller pitch. Primary control in all modes of flight (hover / low-speed, transition, airplane-mode) is governed via an airspeed scheduled mixing scheme described in detail in (Refs. 27,30). The mixer computes an affine mapping between the primary control axes (roll, pitch, vertical thrust, yaw, and longitudinal thrust) to the 11 control effectors (4 lift rotor RPMs, cruise propeller pitch, 2 ailerons, 2 elevators, and 2 rudders). The gains and biases in the airspeed schedule phase out the lift rotors and blend in fixed-wing control deflections in such a way that the aircraft is trimmable and controllable throughout the flight envelope.

From low-speed forward flight through the transition region, a Lift + Cruise configuration does not have a unique trim. This is partly because the controller can use different combinations of lift rotor and control surface deflections to balance the moments on the aircraft. However, the control mixing schedule fixes this control distribution. Even with a fixed mixing schedule, the pilot can use different combinations of propeller thrust and aircraft pitch attitude to balance longitudinal forces, resulting in a range of viable trim conditions. For control design and analysis, a nominal pitch attitude schedule is used from 20-80 knots, where the aircraft transitions from a 3 deg nose up pitch attitude (the trim pitch attitude required in hover) to a 6 deg nose up attitude at 80 knots (which is approximately the trimmed pitch attitude

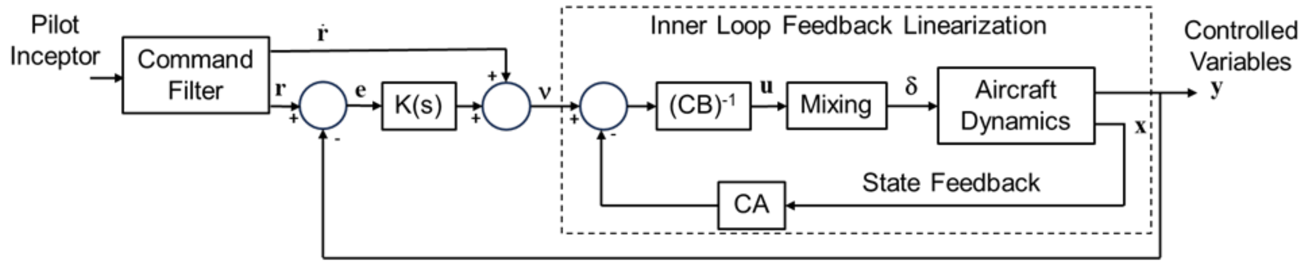

Figure 9. Dynamic Inversion Controller (Ref. 31)

required in airplane mode at 85 knots). Linear models used in control design are generated along this nominal trim schedule, and used for control design and initial HQ analyses, but going forward the HQ analysis must be cognizant of the fact that the pilot will be able fly to off-nominal trims in the absence of any automation.

3.2. Baseline Aircraft Flight Controls

The flight controller design is based on Dynamic Inversion (DI). Linearized models of the aircraft dynamics are generated at different airspeed across the flight envelope. These linearized models are generated by the simulation model at the nominal trim conditions as discussed above. These linear models are reduced to 8-state rigid body models of the aircraft velocity, angular rate, and pitch/roll attitude dynamics. The DI scheme uses full-state feedback (the 8 rigid body states above are assumed measured / estimated) to perform a feedback linearization. The feedback linearization loop converts the aircraft model into a system de-coupled integrators (approximately) which can then be made to follow a prescribed command filter (a.k.a. reference model) by feeding it the first derivative of the commanded state. The command filters govern response to pilot commands, and thus can be tuned to meet desired HQ specifications related to pilot input. In addition, a set of simple PID compensators are used to reject disturbances and to achieve prescribed error dynamic, as discussed in (Ref. 28). These PID compensators can usually be constant gains (no gain scheduling) since the variation of aircraft dynamics is handled by the airspeed-scheduled linear models in the feedback linearization loop. The PID gains can be tuned to minimize disturbance due to modelling error, reject disturbances, and meeting stability requirements. The scheme is well-suited for HQ studies, since it is relatively easy to independently tune response to pilot input and disturbance rejection / stability margin trade-offs. Figure 9 shows a schematic of the overall controller. A full detailed description can be found in (Ref. 31).

For the baseline AFCS, the controller is designed to achieve Attitude Command / Attitude Hold (ACAH) response type in roll and pitch in hover and low-speed flight. The yaw and vertical axis follow heading and height rate response respectively. The command models are summarized in Table 1, its parameters, and the error dynamics parameters used to select PID gains were determined per the method in (Ref. 28).

Table 1. DI Controller Command Models

Axis	Command Model
Roll and Pitch	$\frac{K\omega_n^2}{s^2+s\zeta\omega_n s+\omega_n^2}$
Vertical	$\frac{K}{\tau s+1}$
Yaw	$\frac{K}{\tau s+1}$

4. RAINFLOW COUNTING AS A METRIC

In these initial investigations, it was found that rainflow counting algorithms can be applied to this problem to provide quantitative metrics that provide insight into the performance of a controlled aircraft system, agnostic to the level of automation.

4.1. Rainflow Counting Background

A full description of rainflow counting algorithms is beyond the scope of this paper, but a brief explanation is given, while full details can be found in ASTM E1049-85 (Ref. 13). Figure 10 shows basic terminology as defined in (Ref. 13). For applications beyond load data, the “Reference (Ref) Load” can be replaced with any other nominal reference. In the cases presented here, this would be the reference trajectory (or position) error, equal to zero.

Rainflow counting is done in 4 main steps,

- Hysteresis filtering.
- Peak-Valley filtering.
- Binning.
- Point counting.

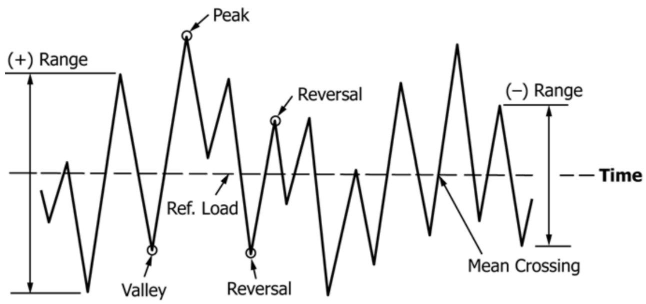

Figure 10. Basic Rainflow Terminology (ASTM E1049-85 (Ref. 13))

Hysteresis filtering is used to set a threshold of cycle size, essentially eliminating cycles smaller than the minimum set by the user. Peak-Valley filtering is used to identify the signal reversals. Binning discretizes the values of the peaks and values to various "buckets." Finally, point counting represents the bulk of the algorithm and where rainflow cycle properties are identified from the signal.

For this study, the rainflow algorithm *rainflow()* built into MATLAB (Ref. 32) (Signal Processing Toolbox) was utilized to generate the cycle counts. Range pairs of cycles counts can be visualized by rotating the filtered signal 90 degrees (as illustrated by transformation the of the data in Figure 11 into Figure 12) and imagining rain flowing down a "roof." As the "rain" cascades down, various rules are used to determine when rain is terminated, and the value-pairs recorded for each half-cycle.

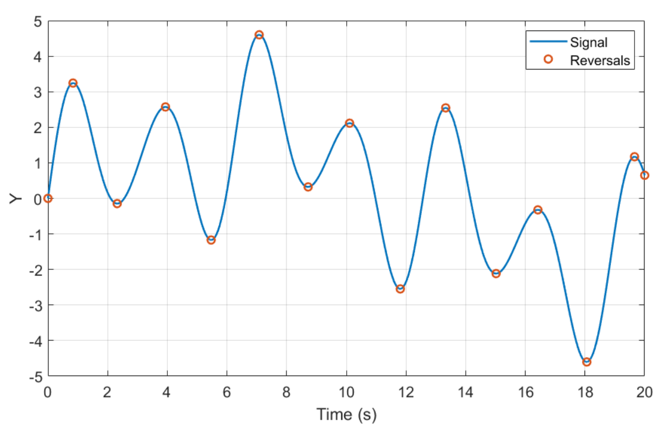

Figure 11. Error Signal Cycle Reversals

Below demonstrates how the rainflow counting algorithm can be applied to a generic time varying signal. The example signal Figure 11 was constructed using several summed sine waves, $y = 1.75sin(0.25t) + sin(t) + 2sin(2t) + 0.25sin(3t)$. It should be noted that the methodology does not make any assumption about the structure of the signal, nor requires anything about the smoothness or differentiability, and therefore can be applied to any time-varying signal. Figure 12 shows the signal after filtering and binning, and rotation has been applied, thus giving the characteristic "rain flow" appearance.

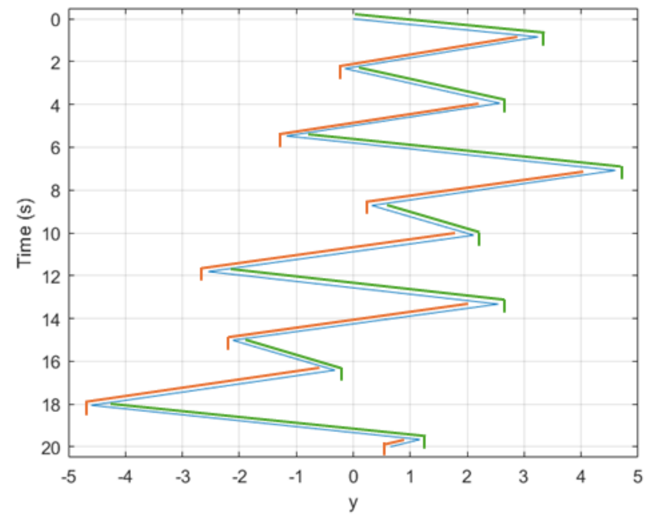

Figure 12. Data Filtered and Rotated 90° to Form "Roof" for "Rain" to Flow Down

Figure 11 shows an example error signal for with the reversals marked. The range, mean, and count of each cycle are computed, along with the start and end time. These identified cycles (results summarized in Table 2) are not exclusively sequential with respect to time, but also capture larger trends (such as biases, or "low frequency" content) in the data that may span several smaller cycles. Following this step, the resulting data can be displayed using a 2-dimensional scatter plot, giving qualitative insight into both the mean and range of aircraft excursions from the reference trajectory.

4.2. Application to VTOL Aircraft

In the cases explored here, the aircraft states can be compared against a reference trajectory and cycle counts of the tracking error can be computed. The basic concept is to see how well the aircraft is tracking a reference trajectory by looking at the tracking error, but more specifically looking at the range and mean of the oscillations of that error signal. This can then be related back to the adequate and desired bounds of the HQTE. The primary benefit with this approach is that is it allows for an easy way to quantify the relative frequency and intensity of excursions from the reference trajectory, as opposed to only looking at time within the prescribed desired and adequate performance regions. This is especially important as the aircraft flight controls continue to be developed with increasing automation.

Table 2. Example Signal Rainflow Cycle Counting Results

Cycle #	Count	Range	Mean	Start Time (s)	End Time (s)
1	0.5	3.24	1.62	0.00	0.84
2	1.0	2.72	1.21	2.32	3.94
3	0.5	4.41	1.04	0.84	5.47
4	1.0	1.79	1.22	8.72	10.11
5	0.5	5.77	1.72	5.47	7.08
6	1.0	1.79	-1.22	15.02	16.42
7	1.0	5.09	3.59	11.81	13.33
8	0.5	9.20	3.82	7.08	18.06
9	0.5	5.77	-1.71	18.06	19.66
10	0.5	0.52	0.91	19.66	20.00

The first step in application of the novel rainflow counting based metric is the computation of the error signal. That is, the difference between the reference signal that the pilot is attempting to track and the actual aircraft attitude (or position).

$$error = y - y_{ref} \tag{1}$$

In Equation 1, y represents the actual state and y_{ref} represents the reference trajectory that the pilot (or autonomous system) is attempting to track. In the case of a Precision Hover type HQTE the error might represent the distance the aircraft is either fore/aft or laterally from the center of the hover box, and in a sum-of-sines task, y_{ref} would be the SoS reference signal.

5. ANALYSIS USING HQTE

The methodology discussed above can be applied to any single axis of a task that has a defined reference trajectory. In displaying the results, it is useful to have an overlay of regions of "goodness" with the cycle scatter chart to easily distinguish the quality of each run. While there are many ways to determine the regions, the method chosen here is based on the size of the adequate and desired bounds of the MTE/HQTE being analyzed. The mean and range of each cycle was normalized by the size of the adequate bound of the task. The region of "adequate" in the cycle-space can then be noted by a triangle extending from negative 1 to positive 1 on the mean-axis, and from 0-2 on the range axis. This shape might seem counter-intuitive at first, but can be found with the following two questions. 1) "What is the largest mean value a cycle can have (assuming zero peak-to-peak range) without violating the adequate state bound?" and, 2) "What is the largest peak-to-peak [range] a cycle can have (assuming zero mean) without violating the adequate state bound?" The answers to these questions are the values given above (Mean ±1, Range 0-2), which are then connected linearly to form a triangle. This outer region is indicated by the yellow patch in Figure 13. While the inner green patch in Figure 13 is defined by the ratio of the size of the desired bound to the adequate bound. It should be noted that these "bounds" are based on the adequate and desired regions of the task, but they do not represent the same metric.

A score can be given (shown in the next section) to give one quantitative measure of performance. This score is determined by calculating what percentage of half-cycles are in each of the three regions (Region 1: Green, Region 2: Green+Yellow, Region 3: Red).

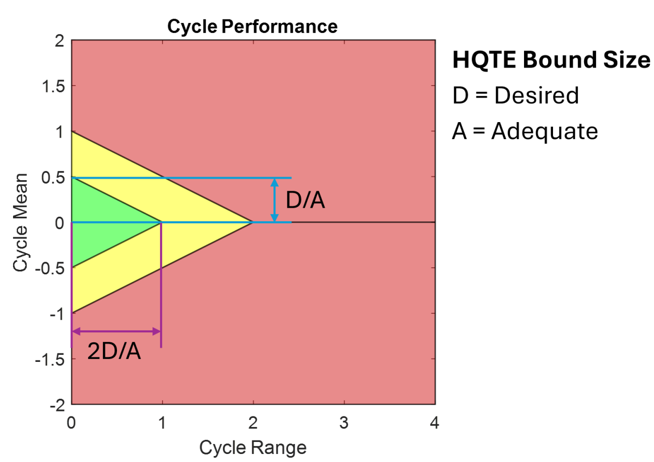

Figure 13. Suggested Rainflow Boundaries

Two assumptions are implied with the setup,

1. The sizes of the adequate and desired bounds are symmetric about the reference trajectory (or position).
2. The sizes of the adequate and desired bounds are constant for the entire portion of the task analyzed.

It is possible these assumptions could be eliminated with adjustments to the normalization, but for the current study they were not deemed to be an issue.

The test pilot contracted for these trials has 40 years of experience flying rotorcraft, airplanes, and powered lift aircraft, 27 years of which were flight test of military rotorcraft and tiltrotors. The pilot also has extensive experience in research flight simulation for flight control development and handling qualities assessment.

5.1 Sum-of-Sines HQTE

Sum-of-Sines is a popular task used in the handling qualities evaluation of rotorcraft. The tight closed-loop nature allows for the effective evaluation of the aircraft control and sensitivity characteristics, inceptor feel system, along with the identification of bobble or Pilot Induced Oscillation (PIO) tendencies. The task is driven by a command signal constructed from the summation of seven sines waves, whose properties can be found in Table 3. Performance requirements for the Pitch SoS task are summarized in Table 4, while an example heads-up display element used by the pilot for the tracking feedback is shown in Figure 14 This task was also chosen because the high number of cycles inherent to the task lends itself well to analysis via the rainflow counting algorithms previously discussed.

For this task, three control mode/inceptor configurations were selected. Configuration 1, Attitude Command / Attitude Hold (ACAH) with pitch control on the longitudinal axis of the primary inceptor. Configuration 2, Flight Path Angle (FPA) command on the longitudinal axis of the primary inceptor. Configuration 3, FPA on the vertical axis of the collective, as might be common in a “unified” control scheme (Ref. 33), i.e., the F-35 approach.

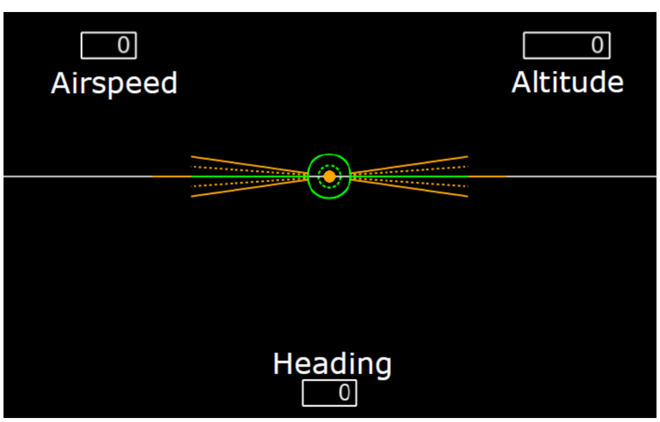

Figure 14. Example Heads-up Display During Sum-of-Sines Task

For each of the three configurations, the pilot was allowed several practice runs to gain familiarisation with the inceptor setup and flight control mode. Following sufficient familiarization an official run for record was performed. After the task was completed, the pilot assigned formal qualitative ratings including the Cooper-Harper Rating scale, Bedford Workload Rating scale, and the Pilot-Induced Oscillation Tendency Rating scale.

Examples of the resulting HQTE performance for Configurations 1, 2, and 3 can be seen in Figures 15, 16, and 17 respectively. All three configurations resulted in satisfactory desired and adequate scores (>50% and >75% respectively) for the pitch error tolerances. However, the Handling Qualities Rating (HQR) and pilot comments recorded expose differences and deficiency with each configuration. As expected, the baseline ACAH configuration allowed for the highest performance of the pitch tracking task, and received a Cooper-Harper rating of 4. Configuration 2, with FPA control on the longitudinal axis of the center-stick inceptor still resulted in reasonable performance but because the flight path angle control does not directly correspond to pitch attitude, it was more difficult for the pilot to track the reference signal, resulting in a lower percentage of time spent in the adequate and desired regions, and a was awarded a slight worsened HQR of 4.5. The third configuration, still used a FPA control mode, but was moved to the vertical axis of the left-hand collective. The scheme was deemed “quite deficient” by the pilot, and was given the lower rating of the three configurations with a HQR 5.

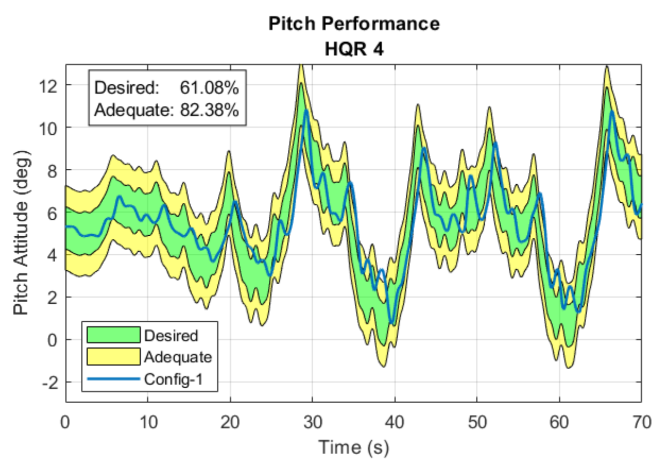

Figure 15. Pitch Sum-of-Sines Performance, Configuration 1

Using the techniques discussed in the previous section, the rainflow counting algorithms were applied to the same three recorded runs. The results are shown in Figures 18, 19, and 20, dubbed as “Cyclograms.” It is immediately apparent that for the cases presented here the Region 1 and Region 2 scores are correlated perfectly with the Cooper-Harper ratings (decreased percentages corresponding to worse HQR), even more so

Table 3. Sum-of-Sines Reference Signal Properties

	1^{st}	2^{nd}	3^{rd}	4^{th}	5^{th}	6^{th}	7^{th}
ω (rad/s)	0.314	0.523	0.837	1.361	2.199	3.560	5.760
Amplitude (deg)	2.493	1.793	1.216	0.766	0.487	0.303	0.188

Table 4. Sum-of-Sines HQTE Performance Requirements

	Desired	Adequate
Pitch: at least X of the scoring time within Y pitch attitude error tolerance:	50%, ±1°	75%, ±2°
PIO Considerations	No PIO tendencies	No divergent PIO tendencies
Inter-axis coupling shall not be...	Undesirable	Objectionable

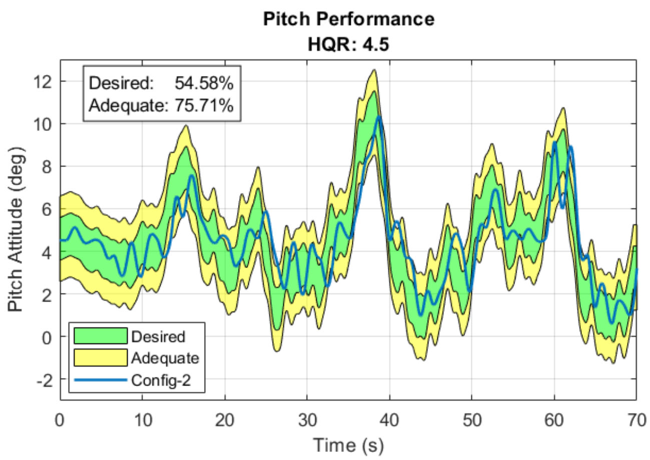

Figure 16. Pitch Sum-of-Sines Performance, Configuration 2

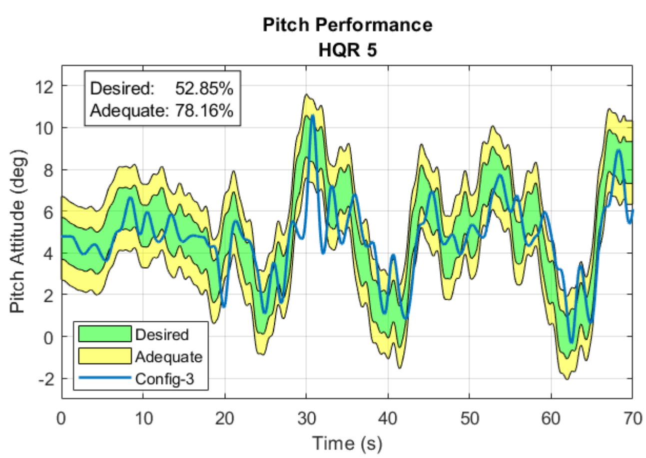

Figure 17. Pitch Sum-of-Sines Performance, Configuration 3

than the desired and adequate scores of the HQTEs (Configuration 3 showed a slightly better adequate score over Configuration 2 even though it was given a worse Cooper-Harper rating in the HQTE). While the difference in adequate score is minor, this shows that the region setup and scoring method of the Cyclograms is justified and should be explored further in future studies. Table 5 shows the different scores outputted by the HQTEs and the Cyclograms, along with the HQR for each configuration tested.

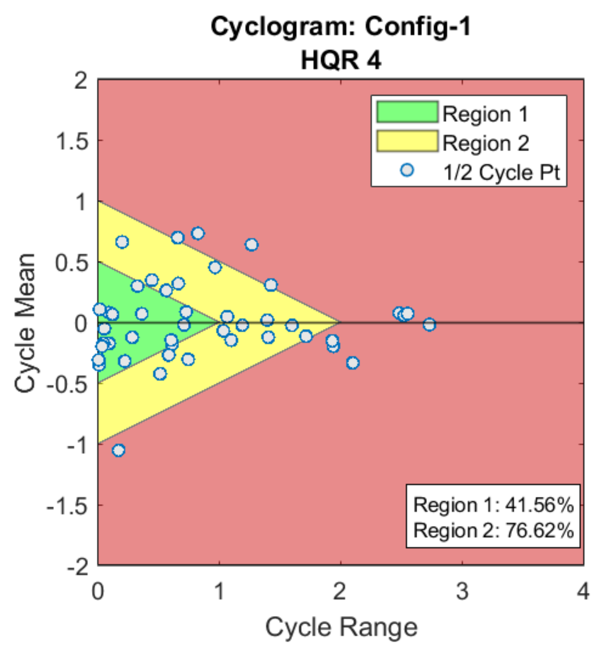

Figure 18. Pitch Sum-of-Sines, Configuration 1

In an ideal tracking case, all scatter points would fall at the origin (0,0). This is because a perfectly tracked reference signal would have zero range error and zero mean error. By visual inspection, Figures 18–20 illus-

Table 5. Sum-of-Sines HQTE Score Comparison

Configuration #	Desired	**Region 1**	Adequate	**Region 2**	HQR
1 - ACAH	61.1	41.6	82.4	76.6	4
2 - FPA	54.6	35.7	75.7	72.9	4.5
3 - FPA (unified)	52.9	18.0	78.2	60.7	5

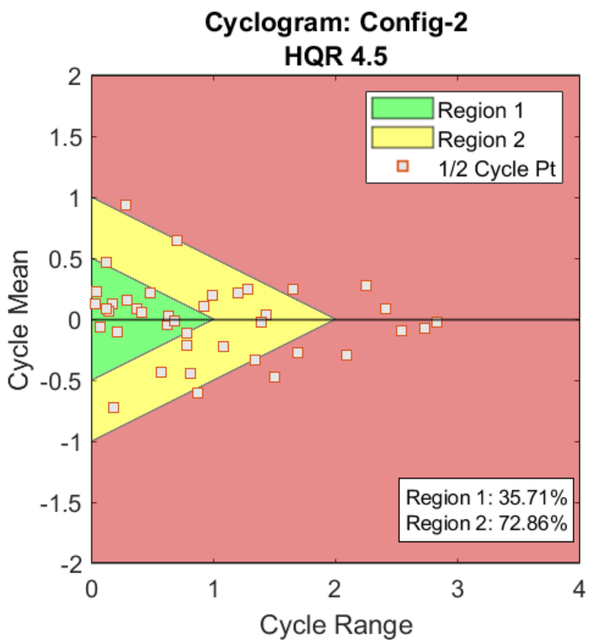

Figure 19. Pitch Sum-of-Sines, Configuration 2

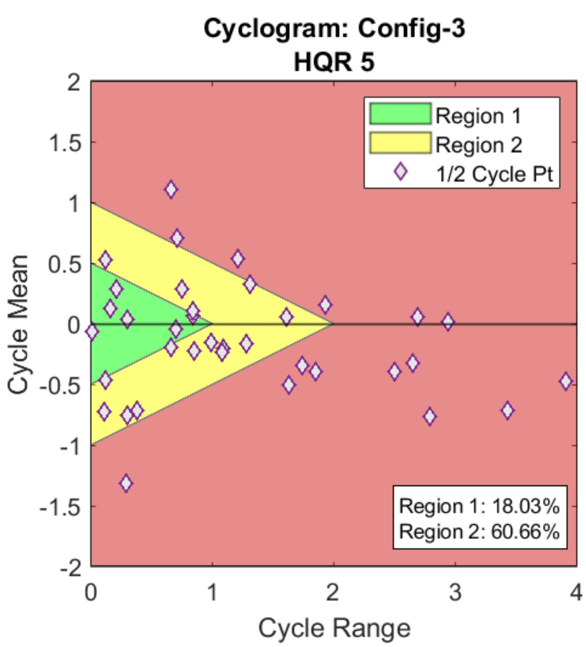

Figure 20. Pitch Sum-of-Sines, Configuration 3

trate how the scatter of half-cycles spreads out away from this ideal point with worsening HQR. This makes sense as worse handling qualities are often associated with lower tracking precision and increased workload.

One item that has not been included in the discussion thus far is pilot comments, and this is where Cyclograms can provide a powerful complement to the HQTE performance plots. For the baseline case (Configuration 1) the pilot commented that stick forces were "manageable and controllable." Figure 18 shows 42% of half-cycles were located in Region 1, with 77% falling within Region 2, recalling that Region 2 also includes all of Region 1 for the purpose of the percentage calculations. In Configuration 2 the pilot indicated that "Some bobble is present when moving through the detent. FPA seems adequate for the task, but ACAH is preferred." This is backed up by the Cyclogram in Figure 19 which shows more points shifted from Region 1 (green) to Region 2 (green+yellow) and beyond, indicating more overshoot and difficulty tracking the center-line of the reference signal. Finally in Figure 20 the percentage of half-cycles that fell in Region 1 was the lowest of all three configurations at just 18%, with 61% falling in Region 2. During this run, the pilot commented that "[Configuration 3] is quite deficient. Attempted to increase gain to improve score, this resulted in more overshoot and less performance." Looking at the time history (Figure 17) this additional gain and overshoot is not readily apparent. However, looking at the Cyclogram in Figure 20, it becomes immediately obvious that the cycle range is much greater than the previous configurations (x-axis) indicating large corrections and overshoot that would be difficult to notice otherwise. This kind of analysis will be more important than ever as increased levels of automation are used to control the aircraft, and pilot comments become less available or more general.

5.1.1. Additional Analysis One of the other strengths of the proposed approach is that data from different runs that cannot be overlaid in the time-domain can be overlaid on a Cyclogram. Take for example, Sum-of-Sines runs, which often are not started at the same point in the signal (differing initial time). In other words, for a reference signal $y_{SoS} = \sum_{i=1}^{7} A_i sin(w_i t)$, the starting time t_0 is not often consistent from run to run. This inconsistency is a good thing from a handling qualities evaluation perspective, as the pilot is not seeing the exact same version of the reference signal but the underlying signal properties are unchanged. However, this can make qualitative analysis more difficult since the reference signal is different from run-to-run. Because the Cyclogram is not displayed with respect to time, data from multiple runs can always be overlaid (even overlaying runs from different HQTEs entirely is made possible). Figure 21 illustrates this by overlaying the three results from the three configurations tested. Once again, the increasing spread of the different configurations correlates perfectly with the change in Handling Qualities Ratings.

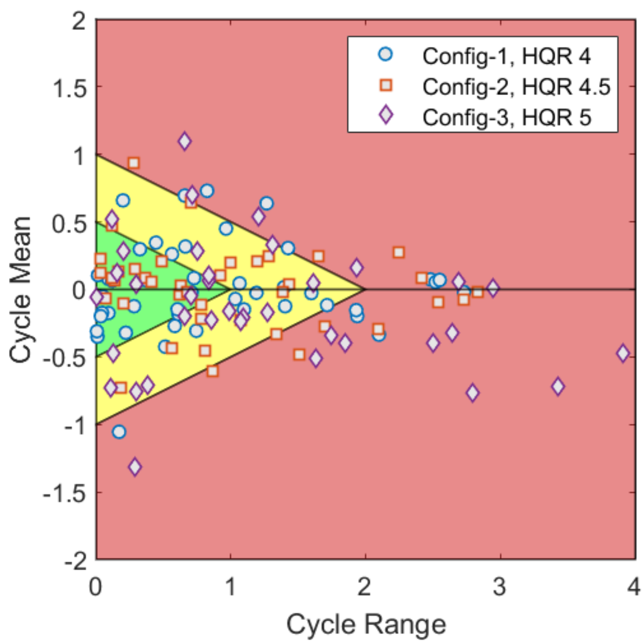

Figure 21. Pitch Sum-of-Sines Cyclogram (All Configurations)

Numerical and discrete data that is not explicitly time- or frequency-domain bound, can often be further analyzed using histograms and empirical cumulative distribution functions (eCDF). An eCDF provides a way to view how much of a data set falls below a certain threshold, and can easily be computed using the equation,

$$
\begin{aligned}
F_n(y) &= \frac{\text{number of elements in the sample} \leq y}{n} \\
&= \frac{1}{n}\sum_{i=1}^{n} I_A(y_i \leq y) \qquad (2)
\end{aligned}
$$

where I_A is the indicator of event I_A (Ref. 34). In the case here, two eCDFs can be generated. The first displays the cumulative probability that the half-cycle range is below a given value (Figure 22), and the second displays the cumulative probability that the half-cycle mean is below a given value (Figure 23). In Figure 23, a perfectly tracked signal would appear like a step-function, going directly from (0,0) to (0,1), then across to (4,1), and so, any case that more approximates this ideal step function is a better performing case. In Figure 22 it can be seen that at each major boundary (green, yellow, red corresponding to Regions 1, 2, and beyond, respectively), the configurations with better HQRs have a greater portion of points in the regions of lower cycle range values.

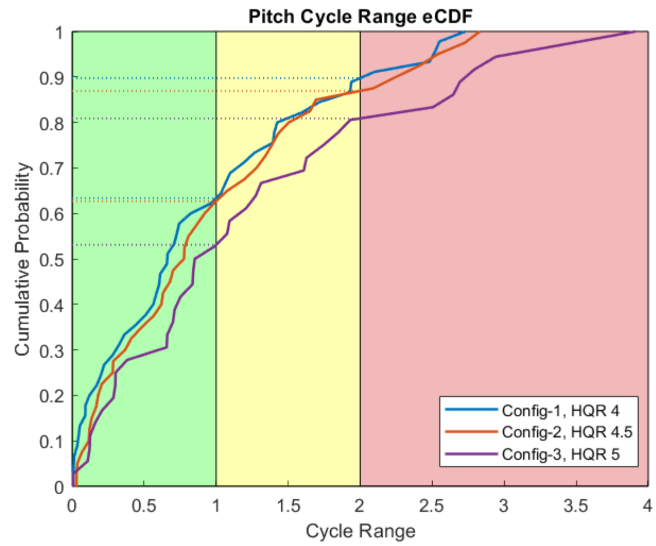

Figure 22. Pitch Sum-of-Sines Cyclogram Range eCDF

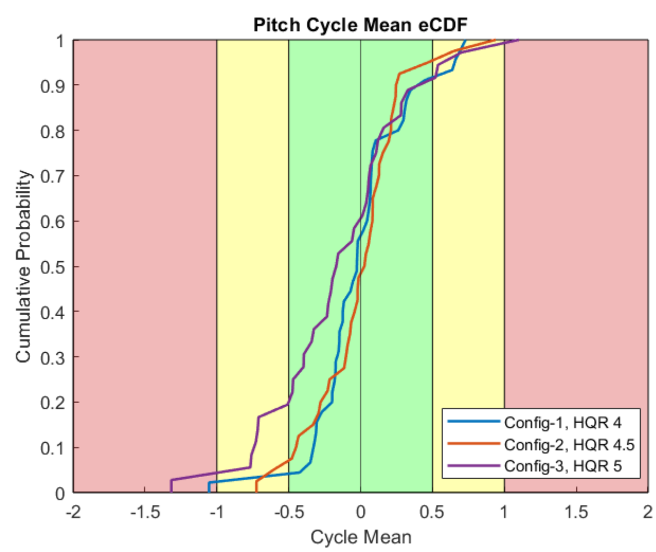

Figure 23. Pitch Sum-of-Sines Cyclogram Mean eCDF

Similarly, the eCDF of cycle mean is computed in a similar way to the eCDF of cycle range. Because the ideal mean value is centered about zero, the bounds appear to sandwich the data from both sides. In this case, the ideal plot would appear as a vertical line going directly from (0,0) to (0,1), so any plots that better approximate a vertical line are deemed to be better. In Figure 23, it can again be seen that the extreme tails of the data corresponding to the poorer rated configurations are stretched further into the regions away from those corresponding to Regions 1 and 2.

While the eCDF plots do not strictly provide more information than the Cyclograms, they can help to identify trends in the data that may not be immediately evident from the 2D scatter-style plots. They also serve to illustrate the advantages of casting the analysis problem into the "cycle-domain," namely, that additionally statically methods can be applied that provide further insight into the aircraft system's tracking capabilities and behavior.

5.2. Precision Hover HQTE and Flying Strategy

The methods described above to analyze HQTE performance using the novel rainflow metrics work very well for cases that have a large number of cycles inherent to the task (such as Sum-of-Sines). However, even if a task has less cycles in the expected signal, useful information can still be provided by these methods. In the example below, two cases of the Precision Hover HQTE are compared. For these two cases the aircraft control mode was set to ACAH. A crosswind of 15 knots from the right was used during both cases. For these test points, the aircraft and environment settings were left unchanged. Instead, the pilot employed two different flying strategies to perform the task. In Run 1, a "nominal" technique was used, i.e., the aircraft was stabilized in the wind before the start of the task using appropriate stick pressure from the pilot. During Run 2, the pilot retrimmed the stick force to account for the wind and before the task was started.

In the Precision Hover task, the aircraft is started in a stationary position downfield at a 45-degree translational offset from the center of the final hover point. The pilot is to initiate the maneuver by accelerating to between 6 and 10 knots, maintaining the 45-degree relative heading between the target hover point and the aircraft. The pilot then attempts to apply a smooth deceleration, followed by a capture of the hover point. A suggested course can be seen in Figure 24.

Figure 25 shows the aircraft ground track performance using the Precision Hover HQTE bounds for both flying strategies. Both techniques appear similar in performance by the time domain metrics and ground track plot (100% Adequate, and >95% Desired for both cases), however, HQRs and pilot comments provide a distinction. Run 1 was awarded Level 2 handling qualities with an HQR 4. The pilot commented that the effect of the wind required "a stronger grip on the stick" and "[a constant] hold right of detent to offset wind, confusing

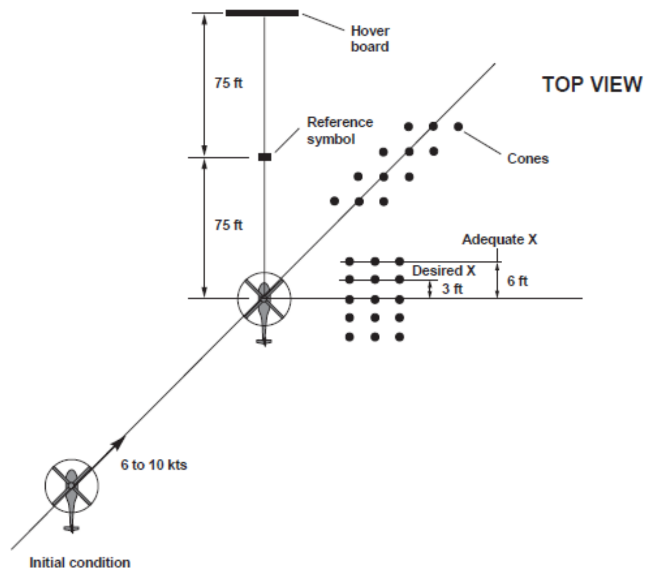

Figure 24. Suggested Course for Precision Hover HQTE (Ref. 4)

capture, and degrading harmony while increasing workload." The pilot also detected a slight tendency to apply oscillation, giving a PIOR 2. In Run 2 (retrim solution) the pilot indicated that it felt almost like there was no wind present and "flew as if there were no winds, did not see [inceptor] harmony issues." For this case, the pilot awarded Level 1 handling qualities with an HQR 3, PIOR 1, showing an improvement in both over the alternative flying strategy.

While the ground track plot in Figure 25 shows some extra movement of the aircraft flown using the nominal flying technique over the retrim strategy, it is difficult to see any significant differences in performance. However, the lateral axis Cyclogram (applied to the maintenance portion of the task) in Figure 26 can provide a deeper insight. It can be seen that the cycle points during Run 1 cover a space greater in magnitude over the data in Run 2, but also are biased with a negative mean. This indicates that the aircraft position was left of center in the hover box, which agrees with a cross-wind from the right, and the pilot comments that a constant right stick was required during the maneuver. Additionally, the smaller cycle range indicates smaller corrections and movements of the vehicle, which show agreement with the pilot comments of a "decreased workload." As was seen in the Sum-of-Sines cases, the tighter clustering of cycle points around the zero mean, and closer to zero range, of the data in Run 1 over Run 2 agree with with both the pilot comments and assigned HQRs.

In a task like Precision Hover it was observed that there were often significantly fewer ½ cycle points on the Cyclogram compared to SoS. This is due to several reasons. First, unlike a task like Sum-of-Sines, the task

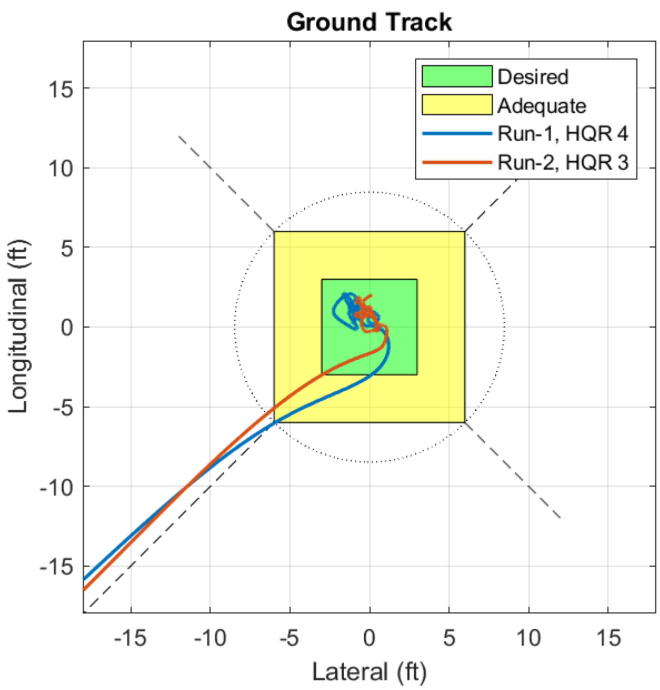

Figure 25. Precision Hover HQTE Groundtrack Performance

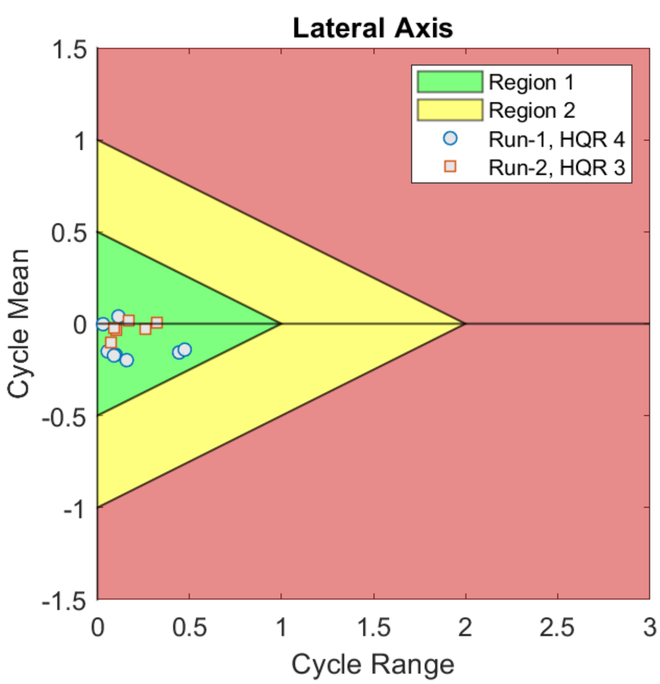

Figure 26. Lateral Axis Cyclogram for Precision Hover HQTE

reference is fixed and not time varying, thus the object of the task is to achieve steady state, and steady state signals appear as only one low frequency cycle point. Second, The maintenance portion of Precision Hover is only 30 seconds, compared to 60 the seconds scoring window of SoS. Figure 27 shows the error signal for the lateral axis Precision Hover runs, illustrating the low number of cycles present in the error signal. However, the reduced number of cycles does not detract from the effectiveness of the method. When fewer cycles are present, each cycle must simply viewed with a higher significance.

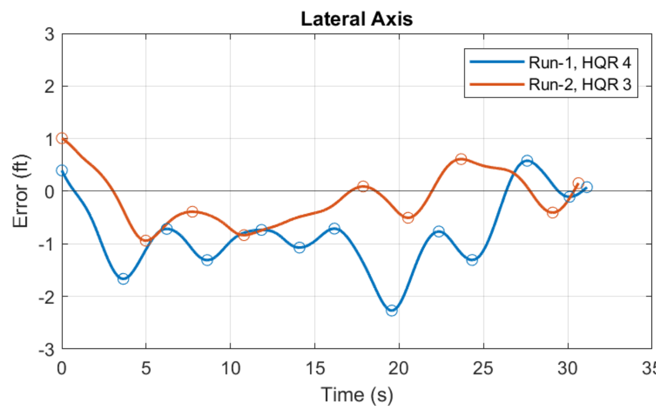

Figure 27. Lateral Axis Error for Precision Hover HQTE

6. CONCLUDING REMARKS

Overall, the novel rainflow counting based metrics (Cyclograms) were found to provide valuable insight into the handling qualities evaluations of a representative VTOL aircraft in simulation. The metrics were found to showcase and trends that could be difficult to identify in traditional analysis methods. They also showed a strong agreement with the pilot comments recorded during testing in a way that is not typically exposed during HQTE evaluations. This insight into vehicle behavior will be of greater importance as the level of autonomy continues to increase and pilot responsibility is shifted from an active role to an evermore passive, or high level, role in "flying" the aircraft. One of the other benefits of the novel analysis methods is the ability to overlay data from runs that are not able to be overlaid in the time domain (such as the SoS task). The ability to overlay data from different HQTEs is also made possible and is an area that future research efforts could benefit. Other areas of focus for future efforts include application to more tasks, the possibility of combining multiple axes into a single Cyclogram, and application of the rainflow-based metrics to other signals, such as inceptor and actuator activity.

Author contact:
Dr. Dakota Musso, dmusso@systemstech.com
Dr. Michael Jones, mjones@systemstech.com

ACKNOWLEDGMENTS

This work was sponsored under SBIR Contract No. 80NSSC22CA098, 'A Certification Means of Compliance Process for Advanced Air Mobility with Increasing Autonomy.' The authors would like to extend thanks to the technical monitor for this project, Jinu Idicula. The authors would also like to thank Marty Shubert of Tiltrotor Flight Test Consulting LLC for his valuable expertise and input during the piloted simulation campaign.

REFERENCES

1. Wing, D. J., Chancey, E. T., Politowicz, M. S., and Ballin, M. G., "Achieving resilient in-flight performance for advanced air mobility through simplified vehicle operations," AIAA Aviation 2020 Forum, 2020.

2. Anon., "Aeronautical Design Standard Performance Specification Handling Qualities Requirements for Military Rotorcraft," Doc. No: ADS-33E-PRF, U.S. Army Aviation and Missile Command, Aviation Engineering Directorate, Redstone Arsenal, Alabama, USA, March 2000.

3. Anon., "Department of Defense Detail Specification on Handling Qualities for Military Ro-torcraft," Doc. No: MIL-DTL-32742, U.S. Army Aviation and Missile Command, Redstone Arsenal, Alabama, USA, March 2023.

4. Klyde, D. H., Mitchell, D., Shubert, M., and Jones, M., "Handling Qualities Test Guide for Powered Lift VTOL Capable Aircraft with Indirect Flight Controls and Operating in Day Time Visual Flight Rules," Doc. No: DOT/FAA/TC-23/59, Federal Aviation Administration, March 2024. DOI: 10.21949/1528262.

5. Miller, J., Jones, M., Klyde, D. H., Heffley, R., and Arencibia, A., "Using Pilot Models to Support Urban Air Mobility Design, Analysis and Certification," AIAA AVIATION 2022 Forum, 2022.

6. Musso, D., Berg, A., and Jones, M., "Using the Task-Pilot-Vehicle (TPV) Approach to Investigate Envelope Protection Design for eVTOL Aircraft," Preceedings of the 80th Annual Forum of the Vertical Flight Society, Monreal, Quebec, Canada, May 12–14, 2024.

7. Klyde, D., Lampton, A., Musso, D., Brand, S., Mitchell, S., Winder, A., Meghdadi, A., and Rhinehart, M., "A Piloted Simulation Study to Investigate the Relationship Between Handling Qualities and Workload," Preceedings of the 79th Annual Forum of the Vertical Flight Society, West Palm Beach, FL, May 12–14, 2023.

8. Lampton, A., Klyde, D., Musso, D., Mitchell, D., and Rhinehart, M., "Further Development of an Approach to Air-craft Handling Qualities Prediction," Presented at AIAA SciTech Forum, Orlando, FL, Jan 8–12, 2024.

9. Klyde, D., Pitoniak, S., Schulze, P. C., Ruckel, P., Rigsby, J., Fegely, C., Xin, H., Fell, W., Horn, J., Ott, C., and Blanken, C., ""Piloted Simulation Evaluation of Tracking MTEs for the assessment of High-Speed Handling Qualities," Preceedings of the 74th Annual Forum of the Vertical Flight Society, Pheonix, AZ, May 14–17, 2018.

10. Memon, W., White, M. D., Padfield, G. D., Cameron, N., and Lu, L., "Helicopter Handling Qualities: A study in pilot control compensation," *The Aeronautical Journal*, Vol. 126, (1295), 2022, pp. 152–186.

11. Lampton, A., and Klyde, D. H., "Power frequency: A metric for analyzing pilot-in-the-loop flying tasks," *Journal of Guidance, Control, and Dynamics*, Vol. 35, (5), 2012, pp. 1526–1537.

12. Jones, M., Klyde, D., Musso, D., Fegely, C., Gillett, L., and Baik, S., "Handling Qualities Evaluations of Active Inceptors with Varying Force-Feel Characteristics," Presented at the VHS Handling Qualities Technical Meeting, Huntsville, AL, Feb 7–8, 2023.

13. Anon, "Standard Practices for Cycle Counting in Fatigue Analysis," Technical Report ASTM E1049-85(2017), ASTM International, West Conshohocken, PA, 2017.

14. Liu, G., Wang, D., and Hu, Z., ""Application of the Rain-flow Counting Method in Fatigue," Proceedings of the 2nd International Conference on Electronics, Network and Computer Engineering (ICENCE 2016), 2016.

15. Amzallag, C., "Standardization of the Rainflow Counting Method for Fatigue Analysis," *International Journal of Fatigue*, Vol. 16, (4), 1994, pp. 287–293.

16. Regassa, Y., and Lemu, H. G., "Damage Assessment of Crack Growth Through Numerical Modelling and Rain Flow Counting Method," *Olympiad in Engineering Science*, Springer, 2023, pp. 268–279.

17. Ghemari, Z., "Navigating Fatigue Analysis with Rain flow Counting: A Practical Overview," *Nov Joun of Appl Sci Res*, Vol. 1, 2024, pp. 01–06.

18. Cheng, T., Lu, D. D.-C., and Siwakoti, Y. P., "Circuit-Based Rainflow Counting Algorithm in Application of Power Device Lifetime Estimation," *Energies*, Vol. 15, (14), 2022, pp. 1–13. DOI: 10.3390/en15145159.

19. Fioriti, D., Scarpelli, C., Pellegrino, L., Lutzemberger, G., Micolano, E., and Salamone, S., "Battery lifetime of electric vehicles by novel rainflow-counting algorithm with temperature and C-rate dynamics: Effects of fast charging, user habits, vehicle-to-grid and climate zones," *Journal of Energy Storage*, Vol. 59, 2023, pp. 106458.

20. Jacobs, C., Yellowley, C., Nelson, D., and Donahue, H., "Analysis of time-Varying Biological Data Using Rainflow Cycle Counting," *Computer Methods in Biomechanics and Biomedical Engineering*, 2000, pp. 31–40.

21. Klyde, D. H., Schulze, P. C., Mitchell, D. G., Sizoo, D., Schaller, R., and McGuire, R., "Mission task element development process: An approach to FAA handling qualities certification," AIAA Aviation 2020 Forum, 2020.

22. Cooper, G. E., and Harper, R. P., *The use of pilot rating in the evaluation of aircraft handling qualities*, National Aeronautics and Space Administration, 1969.

23. Roscoe, A., and Ellis, G., "A Subjective Rating Scale for Assessing Workload in Flight. A Decade of Use," *Royal Aerospace Establishment Technical Report TR90019, Farnborough, UK*, 1990.

24. DiFranco, D. A., *Flight investigation of longitudinal short period frequency requirements and pio tendencies*, Air Force Flight Dynamics Laboratory, Research and Technology Division, Air . . . , 1967.

25. Hindson, W., SCHROEDER, J., and ESHOW, M., "A pilot rating scale for evaluating failure transients in electronicflight control systems," 17th Atmospheric Flight Mechanics Conference, 1990.

26. QtGroup, "Qt Quick 6.7.2 Documentation," *Qt Quick*, August 8, 2024, https://doc.qt.io/qt-6/qtquick-index.html.

27. Mukherjee, B., Jue, A., Theron, J. P., Brentner, K. S., Greenwood, E., and Horn, J. F., "Investigation of departure transition noise for lift-plus-cruise eVTOL aircraft," Proceedings of the 79th Annual Forum of the Vertical Flight Society, West Palm Beach, FL, 2023.

28. Theron, J. P., Horn, J. F., and Wachspress, D. A., "An integrated simulation tool for e-vtol aeromechanics and flight control analysis," Aeromechanics for Advanced Vertical Flight Technical Meeting 2020, Held at Transformative Vertical Flight 2020, 2020.

29. Güner, F., "A Multirotor Inflow Model Based on Combined Momentum Theory and Simple Vortex Theory (CMTSVT) for Flight Simulations," Proceedings of the 78th Annual Forum of the Vertical Flight Society, Fort Worth, TX, May 10–12, 2022., 2022.

30. Theron, J. P., Horn, J. F., Wachspress, D. A., and Enciu, J., "Nonlinear dynamic inversion control for urban air mobility aircraft with distributed electric propulsion," Vertical Flight Society's 76th Annual Forum and Technology Display, 2020.

31. Horn, J., Grant, L., Musso, D., Vo, E., and Jones, M., "Piloted Simulation Evaluation of Augmented Control Modes and Mode Reversions on an eVTOL Aircraft," Proceedings of the 50th European Rotorcraft Forum, Marseille, France, Sept 10–12, 2024.

32. MathWorks, "MATLAB 9.14.0 (R2023a)," *MathWorks, Inc.*, August 6, 2024, www.mathworks.com.

33. Milz, D., and Looye, G., "Tilt-wing control design for a unified control concept," AIAA Scitech 2022 forum, 2022.

34. Ramachandran, K. M., and Tsokos, C. P., *Mathematical statistics with applications in R*, Academic Press, 2020.